Equation of State, Sound Speed, and Reshock of Shock-Compressed Fluid Carbon Dioxide

L. E. Crandall,[1,2] J. R. Rygg,[1,2,3] D. K. Spaulding,[4] M. F. Huff,[1,2] M. C. Marshall,[5] D. N. Polsin,[1] R. Jeanloz,[6] T. R. Boehly,[1] M. Zaghoo,[1] B. J. Henderson,[1,2] S. Brygoo,[7] P. M. Celliers,[5] J. H. Eggert,[5] D. E. Fratanduono,[5] A. Lazicki,[5] M. Millot,[5] and G. W. Collins,[1,2,3]

[1]Laboratory for Laser Energetics, University of Rochester
[2]Department of Mechanical Engineering, University of Rochester
[3]Department of Physics and Astronomy, University of Rochester
[4]University of California, Davis
[5]Lawrence Livermore National Laboratory
[6]University of California, Berkeley
[7]Commissariat à l'energie atomique et aux energies alternatives, France

Mechanical equation-of-state data of initially liquid and solid CO_2 shock compressed to terapascal conditions are reported. Diamond–sapphire anvil cells were used to vary the initial density and state of CO_2 samples, which were then further compressed with laser-driven shock waves, resulting in a data set from which precise derivative quantities including Grüneisen parameter and sound speed are determined. Reshock states were measured to 800 GPa and map the same pressure–density conditions as the single shock using different thermodynamic paths. The compressibility data reported here do not support current density-functional-theory (DFT) calculations but are better represented by tabular equation-of-state models.

The covalent double bonds that bind the atoms in a CO_2 molecule at ambient conditions are among the strongest of chemical bonds, but at pressures reaching tens of GPa, the compression energy becomes comparable to this bonding energy (hundreds of kJ/mol) and the previously stable molecule exhibits complex chemical behavior.[1,2] Laser-heated diamond-anvil cell experiments have characterized the solid phase diagram of CO_2 up to 120 GPa, which exhibits five molecular crystalline polymorphic phases before transforming into both crystalline and amorphous polymeric phases.[1–7]

The fluid phase diagram of CO_2 has been experimentally explored to 1 TPa (Refs. 8–14) and is proposed to exhibit similar chemical complexity to the solid phase diagram.[15] When shock compressed, molecular liquid CO_2 (Fluid I) is stable up to 40 GPa, above which it transforms into an insulating 3- and 4-coordinated polymeric fluid (Fluid II).[12,15] Above 100 GPa, CO_2 transitions into the Fluid-III phase and begins to ionize.[14] The present work is a study of the Fluid-III phase of CO_2.

The pressure, density, temperature, and reflectivity of shocked CO_2 have been measured to 1 TPa and 93,000 K in Ref. 14. Experimental evidence indicates that CO_2 at the highest pressures and temperatures studied is in a complex bonded state as opposed to the previously predicted[13] fully atomic C, O fluid. This work reports further details of the study presented in Ref. 14, and it additionally reports the experimentally determined Grüneisen parameter and isentropic sound speed of shocked CO_2 and the mechanical behavior of CO_2 under reshock.

The pressure and density results from these experiments are plotted in Fig. 1(a) (triangles); the present measurements support LEOS[16] over current DFT[17] calculations in the high-pressure fluid regime. Variation in initial density was leveraged to measure multiple Hugoniot curves, from which derivative quantities were probed using a difference method.[18] The theoretical Grüneisen parameter is systematically higher than the experimental result, but all curves tend to the ideal gas limit of 2/3. The Eulerian sound speed, plotted in Fig. 1(b), can be directly calculated from the measured Hugoniot and Grüneisen parameter.[19] LEOS 2274 (Ref. 16) shows excellent agreement with our experimental data. This is expected given the good agreement between LEOS 2274 (Ref. 16) and our Hugoniot data. The present work measured four reshock states in CO_2 and shows strong agreement with LEOS, as shown in Fig. 1(c).

To summarize, this work provides additional details on recently published[14] equation-of-state measurements of shock-compressed CO_2 to 1 TPa and 93,000 K from varying initial densities and presents new information on the Grüneisen parameter, sound speed, and reshock behavior of high-pressure shocked CO_2. We find that the compressibility, Grüneisen parameter, and sound speed of shocked CO_2 are well represented by LEOS;[16] this work does not support the extreme curvature in compressibility

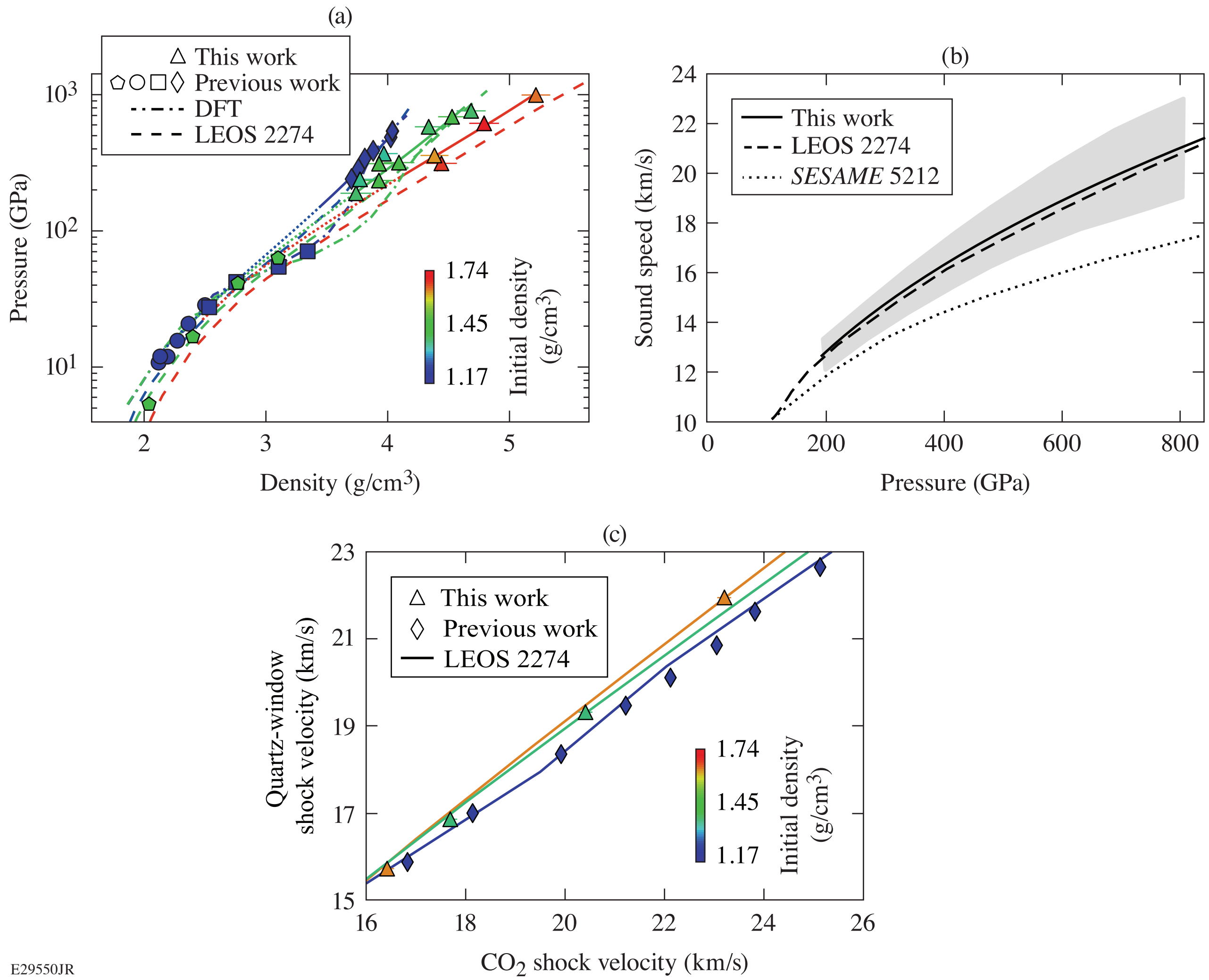

Figure 1
(a) Log pressure versus density for shocked CO_2: OMEGA data (triangles), Sandia Z data[13] (diamonds), and gas-gum data (pentagons),[8] circles,[10] and squares[12]). LEOS[16] (dashed curves) and density functional theory (DFT)[17] (dashed–dotted curves) are also calculated. Solid curves are fits to the OMEGA and Z data; dotted curves extrapolate this fit to lower pressure. The initial density of all data points and curves is given by the color bar. (b) Sound speed of shocked CO_2. This work (solid curve) calculates the sound speed from the measured Hugoniot and Grüneisen parameter. LEOS[16] (dashed curve) shows excellent agreement with these results, while *SESAME* (dotted curve) underpredicts the sound speed. (c) Shock velocity in the quartz window versus shock velocity in the CO_2 sample on either side of their respective interfaces. A reshock is launched back into the CO_2 sample when the shock traverses into the higher-impedance quartz window. These OMEGA data are represented by triangles and the Sandia Z data by diamonds. Solid lines are LEOS curves based on the modeled reshock intersecting with the experimental quartz Hugoniot.[20,21]

modeled by DFT.[17] Notably, lower-pressure gas-gun data support DFT over LEOS. This complexity in the compressibility behavior of shocked CO_2 warrants further study since there is currently a gap between 71 and 189 GPa where no data exist to constrain theory. We report four reshock states of CO_2 and discuss the effect of the Grüneisen parameter on the reshock curve. This work provides significant new benchmarks for theoretical calculations of fluids in the warm-dense-matter regime.

This material is based upon work supported by the Department of Energy National Nuclear Security Administration under Award Number DE-NA0003856, the University of Rochester, the New York State Energy Research and Development Authority, NNSA support to the University of California, Berkeley, and NSF 19-528 Physics Frontier Centers, Award Number 2020249, Center for Matter at Atomic Pressures. This work was performed under the auspices of the U.S. Department of Energy by Lawrence Livermore National Laboratory under Contract DE-AC52-07NA27344 and was supported by the LLNL-LDRD Program under Project No. 12-SI-007.

1. F. Datchi and G. Weck, Z. Kristallogr. **229**, 135 (2014).
2. C.-S. Yoo, Phys. Chem. Chem. Phys. **15**, 7949 (2013).
3. K. D. Litasov, A. F. Goncharov, and R. J. Hemley, Earth Planet. Sci. Lett. **309**, 318 (2011).
4. K. F. Dziubek *et al.*, Nat. Commun. **9**, 3148 (2018).
5. V. M. Giordano *et al.*, J. Chem. Phys. **133**, 144501 (2010).
6. V. M. Giordano, F. Datchi, and A. Dewaele, J. Chem. Phys. **125**, 054504 (2006).
7. H. Shimizu, T. Kitagawa, and S. Sasaki, Phys. Rev. B **47**, 11,567 (1993).
8. V. N. Zubarev and G. S. Telegin, Sov. Phys.-Dokl. **7**, 34 (1962).
9. Zubarev and Telegin[8] report two different initial densities for their solid CO_2: 1.45 and 1.54 g/cm^3. Cited in Schott[10] are "verbal inquires and replies conveyed through C. L. Mader and A. N. Dremin, ca. 1983" that confirm that 1.54 g/cm^3 is a misprint, and the initial density of the data published by Zubarev and Telegin is 1.45 g/cm^3.
10. G. L. Schott, High Press. Res. **6**, 187 (1991).
11. Each measurement of the shock velocity in Ref. 8 is the average of 4 to 12 independent measurements with a 1% to 2% deviation from the mean. Reference 10 similarly presents duplicate measurements of transit times but does not indicate uncertainty. No rigorous systematic uncertainty analysis associated with the data in Refs. 8 and 10 was reported.
12. W. J. Nellis *et al.*, J. Chem. Phys. **95**, 5268 (1991).
13. S. Root *et al.*, Phys. Rev. B **87**, 224102 (2013).
14. L. Crandall *et al.*, Phys. Rev. Lett. **125**, 165701 (2020).
15. B. Boates, A. M. Teweldeberhan, and S. A. Bonev, Proc. Natl. Acad. Sci. **109**, 14808 (2012).
16. C. J. Wu *et al.*, J. Chem. Phys. **151**, 224505 (2019).
17. B. Boates *et al.*, J. Chem. Phys. **134**, 064504 (2011).
18. D. G. Hicks *et al.*, Phys. Rev. Lett. **97**, 025502 (2006).
19. R. G. McQueen, S. P. Marsh, and J. N. Fritz, J. Geophys. Res. **72**, 4999 (1967).
20. M. P. Desjarlais, M. D. Knudson, and K. R. Cochrane, J. Appl. Phys. **122**, 035903 (2017).
21. S. Brygoo *et al.*, J. Appl. Phys. **118**, 195901 (2015).